An improved crack driving force estimation approach for stress-based engineering critical assessment of reeled pipes

Manuscript Details

Manuscript number	TAFMEC_2019_59_R3
Title	An improved crack driving force estimation approach for stress-based engineering critical assessment of reeled pipes
Article type	Research Paper

Abstract

In the study, an improved reference load solution is proposed to determine the reference stress and the J-integral for pipelines subjected to reeling, where the axial strains during installation are typically within the range of 1.5%-3.5%. Accordingly, the reference stress can be directly correlated with the un-cracked remote stress of the component through the loading-independent parameter, λ. The effects of cracked geometries and material properties on the reference stress are systematically investigated, and an empirical formula for the reference stress is provided. The proposed method is validated against various J estimation schemes in the literature. It is concluded that the present reference load solution is able to provide an improved and simplified J-integral estimation for the considered geometries over the full strain range of interest.

Keywords	Reeling; J-integral estimation; Crack driving force; Reference stress; Pipeline.
Manuscript region of origin	Asia Pacific

Corresponding Author	Baoming GONG
Corresponding Author's Institution	Tianjin University
Order of Authors	Yizhe Li, Baoming GONG, Giuseppe Lacidogna, Alberto Carpinteri, Dongpo Wang
Suggested reviewers	zhiliang zhang, Yuh Chao, Xiancheng Zhang, Xiaohui Zhao

Submission Files Included in this PDF

File Name [File Type]

Response to Reviewer R2.docx [Response to Reviewers]

Highlights.docx [Highlights]

Manuscript marked R2.docx [Manuscript File]

To view all the submission files, including those not included in the PDF, click on the manuscript title on your EVISE Homepage, then click 'Download zip file'.

Reply to the Reviewer's comments

Manuscript Number: TAFMEC_2019_59_R2

Title: An improved crack driving force estimation approach for stress-based engineering critical assessment of reeled pipes

Authors: Yizhe Li, Baoming Gong, Giuseppe Lacidogna, Alberto Carpinteri and Dongpo Wang

Reply to Reviewer 2

The authors seem a little reluctant in implementing some of the changes driven by my previous observations. It is generally not enough not convince the Reviewer but also other readers, so I do not understand why they haven't included some of the observations/remarks addressed in their response into the revised article. Essentially, they have basically changed the term "limit load solution" to "reference load solution" throughout the text! Nevertheless, I would like to see Fig. 1 of their response (Maximum acceptable flaw sizes for (a) API 5L X65 steel and (b) API 5L X70 steel) included in the revised text. What is the reason for not including those results? They add much more value and actually show what would be the final application of the methodology addressed in the paper.

The authors have greatly appreciated the suggestions proposed by the Reviewer which have significantly improved the work. The results of Maximum acceptable flaw sizes for (a) API 5L X65 steel and (b) API 5L X70 steel are added in the revised manuscript.

Highlights

- An improved crack driving force estimation approach is proposed for J estimation schemes in circumferentially surface cracked pipes subjected to reeling;
- A geometry and material dependent non-dimensional parameter λ is introduced to relate the reference stress directly to the uncracked remote stress.
- The proposed improved reference stress solution has an explicitly theoretical foundation and is capable to provide a safe and conservative estimation of J-integral for geometries over the full range of interest.

An improved crack driving force estimation approach for stress-based engineering critical assessment of reeled pipes

Yizhe Li [a], Baoming Gong [a,*], Giuseppe Lacidogna [b], Alberto Carpinteri [b] and Dongpo Wang[a]

[a] *Department of Materials Science and Engineering, Tianjin University, Road Weijin 92, 300072 Tianjin, China*
[b] *Department of Structural Engineering, Geotechnics and Building, Politecnico di Torino, Corso Duca degli Abruzzi 24, 10129 Torino, Italy*

*The correspondence E-mail: gongbm@tju.edu.cn

Abstract

In the study, an improved reference load solution is proposed to determine the reference stress and the *J*-integral for pipelines subjected to reeling, where the axial strains during installation are typically within the range of 1.5%-3.5%. Accordingly, the reference stress can be directly correlated with the un-cracked remote stress of the component through the loading-independent parameter, λ. The effects of cracked geometries and material properties on the reference stress are systematically investigated, and an empirical formula for the reference stress is provided. The proposed method is validated against various *J* estimation schemes in the literature. It is concluded that the present reference load solution is able to provide an improved and simplified *J*-integral estimation for the considered geometries over the full strain range of interest.

***Keywords*:** Reeling; *J*-integral estimation; Crack driving force; Reference stress; Pipeline.

Nomenclature	
a	crack depth
c	crack length
D	pipe outer diameter
E	Young's modulus
f_1, f_2	dimensionless parameter
J	J-integral
J_e, J_p	elastic and plastic components of J-integral
K_I	stress intensity factor (Mode I)
K_r	vertical axis of FAD
L_r	horizontal axis of FAD
n	strain hardening exponent
P	remote load
P_L	plastic limit load
R	reeling radius
r	pipe outer radius
t	pipeline wall thickness
α	dimensionless material constant
β_0-β_{10}	fitting coefficients
σ	nominal stress (remote stress)
σ_0,σ_{ys}	yield stress of the material
σ_u	ultimate stress of the material
σ_{ref}	reference stress
ε_0, ε_{ys}	yield strain
ε_{ref}	reference strain
ε_n	nominal strain (remote strain)
λ	non-dimensional factor of reference stress in the study
γ	non-dimensional factor of reference stress by Tkaczyk
Abbreviations	
CDF	crack driving force
CTOD	crack tip opening displacement
ECA	engineering critical assessment
EPRI	electric power research institute
FAC	failure assessment curve
FAD	failure assessment diagram
FEA	finite element analysis

1. Introduction

The reel-lay is widely employed to install submarine pipelines and riser, which allows the entire pipe to be fabricated at onshore by connecting shorter tubular sections through girth welds [1]. During installation, the pipeline is spooled onto a reel at first, then passing through an aligner and a straightener, and final launched to the seabed by unspooling the reel, as schematically shown in Fig. 1. Therefore, the pipeline is subjected to plastic straining often involving more than one cycle. The axial strains developed during installation depend on the pipe and reel diameters but are typically in the range of 1.5%-3.5% [2], which well exceeds the yielding limits of the parent material. To ensure the integrity of submarine pipeline systems, it is mandatory to take into consideration the complex loadings, such as high internal/external pressure combined with bending, tension and even torsion, accompanied by large plastic strains. Meanwhile, the welding defects may be introduced into the girth welds. The state of stress resulting from these loads, in combination with other factors such as crack and pipe geometry, material properties etc., may lead to initiation of fracture from welding defects or cross-sectional instability and collapse of the pipe.

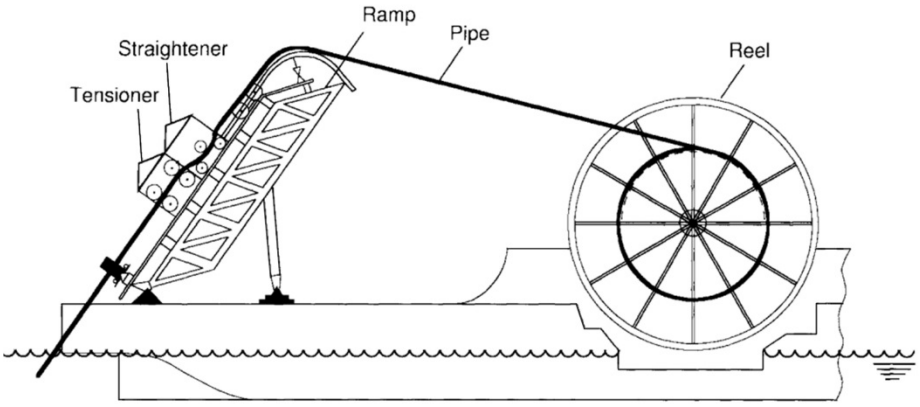

Figure 1 Illustration of offshore reel-lay technique [3].

Fracture mechanics-based assessment procedures, such as BS 7910 [4] and DNVGL-RP-F108 [5], are employed to provide defect tolerance of girth welds during installation and operation of offshore pipelines, i.e.

Engineering Critical Assessment (ECA), which provides the rational decisions on monitoring and maintenance rate without compromising the integrity of the girth welds. These assessment methodologies (e.g. BS7910 [4], DNV-OS-F101 [6], API 579 [7]) are essentially developed for load-controlled conditions. However, they do not necessarily provide accurate assessments for pipeline subjected to displacement controlled loading into the plastic regime. For example, API 1104 [8] limits to less than 0.5 % strain and DNV-OS-F101 [6] to less than 0.4 % strain. Therefore, the defect assessment methodologies have been extended recently through the modified stress-based approaches [1, 9] or the strain-based schemes [10-13]. The effectiveness of assessment procedures of cracked pipes and cylinders relies strongly on the accuracy of crack driving forces (CDF) [14], which is usually characterized by *J*-integral and/or crack tip opening displacement (CTOD). Although the substantial advancement in three-dimensional finite element analysis (FEA) nowadays allow a direct calculation of *J* and/or CTOD, the cost of manpower and time is enormous regarding the complexity of the pipeline configurations and loading conditions. Therefore, the established analytical procedures for the CDF estimation are still substantially important in engineering designs.

At beginning, the foundation for fitness for service is essentially based on the reference stress method proposed by Ainsworth [15], which is an extension of the well-known Electric Power Research Institute (EPRI) estimation [16]. Recently, the strain-based procedures have drawn extensively attention due to the strain/displacement-controlled loading nature in pipeline industry [17]. Øtsby et al. [11] and Jayadevan et al. [10] found a simple linear evolution between the applied strain vs. CTOD under both tension and bending conditions. Based on the reference strain approach, Nourpanah and Taheri [18] developed more accurate *J*-integral estimation equations to assess fracture behavior in reeled pipelines. Budden [12, 13] adopted the reference strain method in [19] and extended the stress-based failure assessment diagram (FAD) to the strain-based FAD method. However, since the reference strain is taken as the uncracked value at the location of the crack [19], the application of these methods is limited to a crack depth ratio less than 0.2 ($a/t < 0.2$) to exclude

the significant effect of deeper cracks on the compliance of the structure [13, 20]. Jia et al. [21] proposed an empirical formula to correlate the reference strain to the uncracked strain for severe cracks. However, as indicated by Budden [13], the reference strain estimate of J holds only for certain geometries. Although a factor of 2 is retained to ensure the conservatism of strain-based FAD, the selection of reference strain remains controversial and its application in engineering is still limited [22].

The accuracy of crack driving force estimation in the reference stress method depends highly on the definition of the plastic limit load P_L, through which the geometry and strain hardening dependence of the $h(n)/h(n=1)$ ratio is minimized [15], where $h(n)$ is a dimensionless function of the component geometry and the strain hardening exponent. Several popular reference stress solutions can be found in the literature [23-26]. Among which the limit load solution of Kastner et al. [23] is recommended by DNV-RP-F108 and extensively used for the fracture assessment in the offshore industry. Although Kastner's limit load solutions for defective components are commonly available [24], Tkaczyk et al. [1] pointed out that this approach may lead to inaccurate fracture assessments. Following the optimized reference stress approach in [9], Tkaczyk et al. modified Kastner's limit load solution through a non-dimensional factor γ, which is a function of geometry and hardening exponent n, to $\tilde{P}_L=\gamma P_L$ [1]. Moreover, the limit load solution of Kastner is a function of cracked geometries considering local plastic collapse of surface cracked cylinders, which thus makes the J estimation formula quite complicated. Thus, higher level of required effort still underlies the need of simplified J and CTOD estimation methods in the defect assessments. In addition, the theoretical foundation of the modified limit load solution is still unclear, and the coupling effects of geometry parameters and hardening exponent on the limit load has not been exhausted yet.

In the study, an improved reference load solution is proposed to determine the reference stress and the J-integral for pipelines subjected to reeling with axial strain in the range of 1.5%-3.5%. First, the theoretical background of J estimation schemes is briefly reviewed. A geometry and material dependent parameter λ is

used to relate the reference stress directly to the uncracked remote stress of the component for a wide range of crack configuration and material property. An empirical formula for λ is provided based on the detailed parametric analyses. Finally, the proposed solution is manifested by comparing with various J estimation schemes in the literature.

2. The proposed reference load solution

2.1 Theoretical framework of stress-based J estimation schemes

The path-independent J-integral [27] and crack tip opening displacement (CTOD) [28] are two most important elastic-plastic fracture parameters [29]. For defect assessments of elastic–plastic materials with sufficient toughness, the J-integral can be derived from the HRR stress field solutions [30, 31]

$$\sigma_{ij} = \sigma_{ys}\left(\frac{J}{\alpha\varepsilon_{ys}\sigma_{ys}I_n r}\right)^{1/1+n}\tilde{\sigma}_{ij}(n,\theta) \tag{1}$$

where (r, θ) are the polar coordinates centered at the crack tip; I_n is an integration constant related to hardening exponent n and $\tilde{\sigma}_{ij}(n, \theta)$ are dimensionless stress functions. The J-integral can then be conveniently derived from the above equation in the reference stress method as follows:

$$J = \frac{\alpha\varepsilon_{ys}\sigma_{ys}I_n r}{[\tilde{\sigma}_{ij}(n,\theta)]^{(n+1)}}\left(\frac{\sigma_{ij}}{\sigma_{ys}}\right)^{(n+1)} \tag{2}$$

Since the reference stress method is the most successful J estimation scheme applied in conducting structural integrity assessment for components with cracked defects, a brief overview of the development of the stress-based J estimation approaches is given in this section.

2.2 EPRI J–integral estimation method

The J-integral estimated by the EPRI approach of Kumar et al. [32] begins by considering materials whose true uniaxial stress–strain relationship can by characterized by the Ramberg–Osgood constitutive model

$$\frac{\varepsilon}{\varepsilon_0} = \frac{\sigma}{\sigma_0} + \alpha\left(\frac{\sigma}{\sigma_0}\right)^n \tag{3}$$

where α is a dimensionless material constant, σ is the nominal stress, which is taken as the far-field applied stress of the pipeline in the work, n is the strain hardening exponent, σ_0 and $\varepsilon_0 = \sigma_0/E$ denotes the yield stress

and strain, respectively. Omitting the elastic component, it is approximately given as:

$$\frac{\varepsilon}{\varepsilon_0} = \alpha\left(\frac{\sigma}{\sigma_0}\right)^n \tag{4}$$

According to Kumar et al. [32], the fully plastic component of J-integral can be written as:

$$J_p(a) = \alpha\sigma_0\varepsilon_0 a h(n)\left(\frac{P}{P_L}\right)^{n+1} \tag{5}$$

where a denotes the crack depth; $h(n)$ is a dimensionless function of the component geometry and the strain hardening exponent; the applied load can be determined as $P=2\pi rt\sigma$, and P_L is the normalizing limit load proportional to σ_0. Considering $\alpha=1$ and $n=1$ in Eq. (5), the elastic contribution of J can be expressed as:

$$J_e(a) = \sigma_0\varepsilon_0 a h(n=1)\left(\frac{P}{P_L}\right)^2 \tag{6}$$

J_e can also be calculated directly from the Mode I stress intensity factor K_I :

$$J_e = \frac{K_I^2}{E'} \tag{7}$$

where $E'=E/(1-\nu^2)$ for the plane strain condition and $E'=E$ for the plane stress condition. The total J-integral is the sum of the elastic and plastic components:

$$J(a)=J_e(a)+J_p(a) \tag{8}$$

However, the accuracy of the EPRI method depends highly on the fitting accuracy of the Ramberg-Osgood model [9, 33], and its applicability is limited only to a few configurations, for which the h factors are tabulated [1, 14, 34].

2.3 The modified reference stress method

Ainsworth [15] extended the reference stress approach to materials besides Ramberg-Osgood curve as well as the tabulation of h values, by defining a reference stress:

$$\sigma_{ref}=\frac{P}{P_L}\sigma_0 \tag{9}$$

Substituting Eq. (9) into Eqs. (5) and (6) gives:

$$\frac{J_p(a)}{J_e(a)} = \alpha\frac{h(n)}{h(n=1)}\left(\frac{\sigma_{ref}}{\sigma_0}\right)^{n-1} \tag{10}$$

The reference strain ε_{ref} can be determined as:

$$\varepsilon_{ref} = \varepsilon_0\left(\frac{\sigma_{ref}}{\sigma_0} + \alpha\left(\frac{\sigma_{ref}}{\sigma_0}\right)^n\right) \tag{11}$$

Considering Eq. (10) and Eq. (11), the ratio of plastic and elastic contributions can be obtained as:

$$\frac{J_p(a)}{J_e(a)} = \frac{h(n)}{h(n=1)}\left(\frac{E\varepsilon_{ref}}{\sigma_{ref}} - 1\right) \tag{12}$$

Although the strong dependence of $\frac{h(n)}{h(n=1)}$ on cracked geometries and strain hardening exponent was observed [9], a proper limit load should be selected to minimize the geometrical and material dependence [15]. By assuming $\frac{h(n)}{h(n=1)} = 1$, Eq. (12) becomes:

$$J_p(a) = J_e(a)\left(\frac{E\varepsilon_{ref}}{\sigma_{ref}} - 1\right) \tag{13}$$

By incorporating minor plastic correction terms proposed by Milne et al. [35], the final form of the *J*-estimation approach of BS 7910 [4] is obtained:

$$J(a) = J_e(a)\left(\frac{E\varepsilon_{ref}}{\sigma_{ref}} + \frac{1}{2}\frac{\sigma_{ref}^3}{\sigma_0^2 E\varepsilon_{ref}}\right) \tag{14}$$

and the FAC can be drawn as follows:

$$f(L_r) = K_r = \left(\frac{E\varepsilon_{ref}}{\sigma_{ref}} + \frac{1}{2}\frac{\sigma_{ref}^3}{\sigma_0^2 E\varepsilon_{ref}}\right)^{-\frac{1}{2}} \tag{15}$$

where the horizontal axis $L_r = \frac{P}{P_L}$ measures the proximity to plastic collapse, and the vertical axis K_r represents the proximity to fracture. Eq. (15) is suitable to any material response for the estimation of *J* without the limitation of Ramberg–Osgood material. However, the accuracy of such *J* estimate procedure is strongly dependent on the limit load. Following BS 7910 [4], DNV [5] recommends the limit load solution of Kastner et al. [23] to calculate the reference stress:

$$P_L = 2\pi rt\sigma_0 \frac{(1 - a/t)[\pi - (c/r)(a/t)]}{\pi(1 - a/t) + 2(a/t)\sin(c/r)} \tag{16}$$

where 2*c*, *r*, and *t* are the crack length, pipe outer radius and wall thickness, respectively. The geometry features are schematically illustrated in Fig. 2.

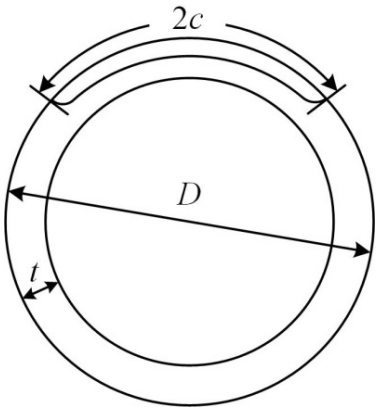

Figure 2 Geometry features of an external circumferential crack.

For a given material and crack configuration, the P_L proposed by Kastner et al. [23] holds constant, whereas the accuracy of such *J*-estimation scheme is questionable [36]. To further eliminate the influence of $h(n)/h(n=1)$ and provide the improved *J*-estimation results, Kim and Budden [9] replaced the limit load P_L with an optimized reference load:

$$\tilde{P}_L = \gamma P_L \tag{17}$$

where parameter γ is a function of geometry and hardening exponent *n*. The optimized reference load is determined as:

$$\frac{h(n)}{h(n=1)}\left(\frac{\tilde{P}_L}{P_L}\right)^{n-1} = 1 \tag{18}$$

Using Eq. (9) and Eq. (18), Eq. (10) is expressed as

$$\frac{J_p(a)}{J_e(a)} = \alpha\left(\frac{P}{\tilde{P}_L}\right)^{n-1} \tag{19}$$

and the parameter γ is expressed as

$$\gamma = \left(\alpha\frac{J_e}{J_p}\right)^{1/n-1}\frac{P}{P_L} \tag{20}$$

which is determined through the elastic and total *J*-integral obtained from linear elastic and elastic–plastic FE analyses.

2.4 The improved reference load solution

Although the optimized reference stress method results in an improved accuracy, the parameter γ is

essentially dependent on the selection of the limit load solution. Since the geometry and material dependence of the reference stress cannot be directly characterized by the parameter γ, the optimized reference load solution can be quite complicated without explicit theoretical foundation. According to Eqs. (16) and (17), P_L is proportional to $2\pi rt\sigma_0$. Therefore, a reference load can be defined as:

$$P_L^R = 2\pi rt\sigma_0\lambda \tag{21}$$

where the dimensionless parameter λ is assumed to be a function of cracked geometry and material property.

Substituting Eq. (21) into Eq. (9), the reference stress can be directly related to parameter λ:

$$\sigma_{ref} = \sigma / \lambda \tag{22}$$

Assuming $\frac{h(n)}{h(n=1)} = 1$, the non-dimensional parameter, λ, can be obtained by substituting Eq. (22) into Eq. (10) as:

$$\lambda = \frac{\sigma}{\sigma_0}\left(\alpha\frac{J_e(a)}{J_p(a)}\right)^{1/(n-1)} \tag{23}$$

The reference stress proposed in the study can be thus understood as the stress of a cracked component, which is directly correlated with the un-cracked remote stress of the component through the geometry and material dependent parameter, λ. The process of the determination of λ is given in the coming section.

3. Determination of λ

According to Eq. (23), the nominal stress σ can be determined in terms of the remote strain, ε_n, with the Ramberg–Osgood model. For reeled pipes, the value of J can be calculated by a simple displacement-controlled J estimation approach proposed by Nourpanah and Taheri [18], and the maximum error is within 2% for the considered strain range ($1.5\% \leq \varepsilon_n \leq 4\%$)

$$\frac{J(a)}{\sigma_0 t} = (f_1\varepsilon_n + f_2) \tag{24}$$

where f_1 and f_2 are functions of material properties and cracked geometries, and tabulated for the specified crack sizes and material properties [18]. The elastic and plastic components of J-integral can be conveniently calculated using Eqs. (7), (8) and (24) as well as the stress intensity factor solution for circumferential surface

cracks recommended by BS 7910 [4]. Then, the value of λ can be determined by Eq. (23). A total of 300 models are presented in the study. The parameters of cracked geometries and material properties are from Nourpanah and Taheri [18] as listed in Table 1.

Table 1 Parameters of geometries and material properties.

Parameter	Value
a/t	0.1, 0.2, 0.3, 0.4, 0.5
D/t	10, 15, 20, 25, 30
$2c/(\pi D)$	0.05, 0.1, 0.15, 0.2
n (σ_0/σ_u)	10 (0.659), 15 (0.757), 25 (0.846)

3.1 Load-independence of λ

Figure 3 shows the evolution of λ versus the applied load (for the particular case of interest, the loading is phrased in terms of applied strain) for a family of $2c/\pi D$, D/t, n, and a/t. It is found that λ is only sensitive to the geometry and material parameters, and approximately load-independent. More specifically, although a nonlinear relationship can be observed between λ and the nominal strain at the lower loading levels, λ is approximately constant in the range $\varepsilon_n \geq 2\%$. Accordingly, the value of λ corresponding to $\varepsilon_n = 4\%$ is chosen as the reference value for one specific crack geometry and material property in Appendix A.

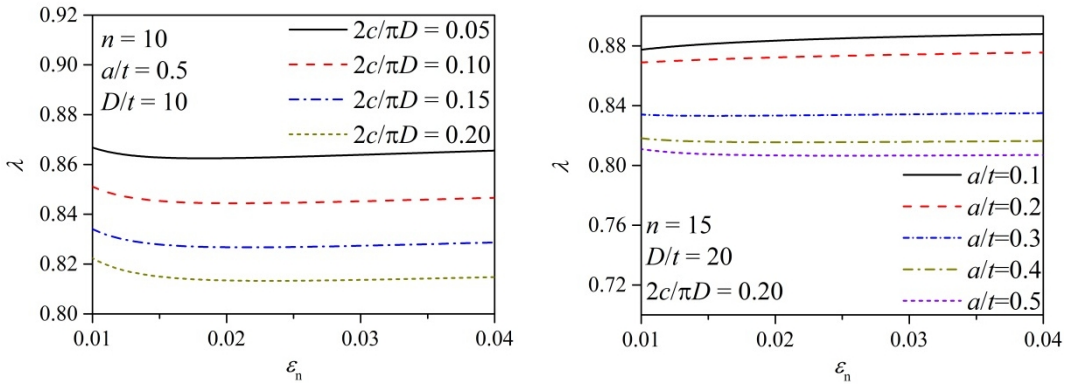

(a) (b)

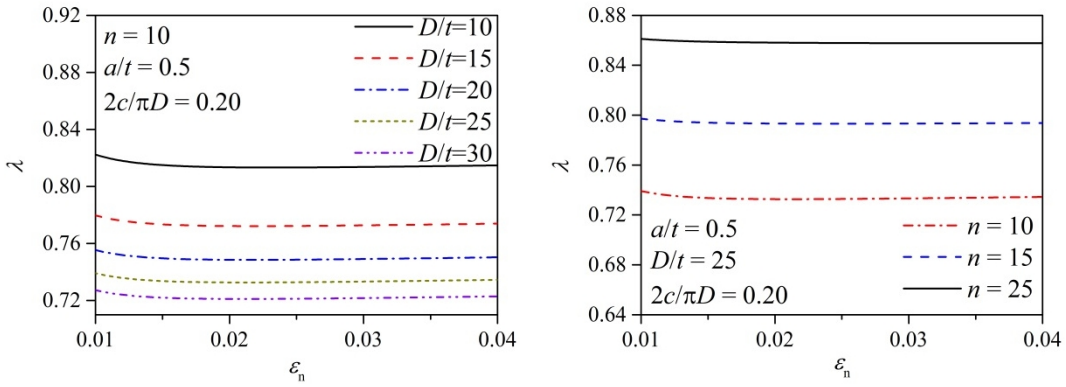

(c) (d)

Figure 3 Evolution of parameter λ versus nominal strain for (a) various $2c/\pi D$ values, (b) various a/t values, (c) various D/t values, and (d) various n values.

3.2 Effects of a/t, D/t, $2c/(\pi D)$ and n on λ

Since the dimensionless parameter λ is a function of cracked geometry and material property as discussed before, it is essential to investigate the effects of a/t, D/t, $2c/(\pi D)$, and n on λ. The results are shown in Figs. 4-6. Figure 4a illustrates that λ is weakly dependent on $2c/\pi D$ for shallow cracks (a/t = 0.1 and 0.2), while strongly dependence on $2c/\pi D$ for deep cracks (a/t = 0.3, 0.4 and 0.5) can be found. As a/t increases, λ decreases significantly with increasing $2c/\pi D$, it is evident that the coupled interactions of $2c/\pi D$ and a/t have strongly influences on λ at large values of $a/t > 0.3$ and $2c/\pi D > 0.1$. The synthesized effect of $2c/\pi D$ and D/t on λ is shown in Fig. 4b. It is observed that a linear evolution of λ versus $2c/\pi D$ can be observed for all the D/t ratios, and the value of λ is much lower for larger D/t at the same $2c/\pi D$. A similar effect of $2c/\pi D$ and n on λ can be observed in Fig. 4c, with a higher λ for the low hardening material (n=25) at the same $2c/\pi D$ ratio.

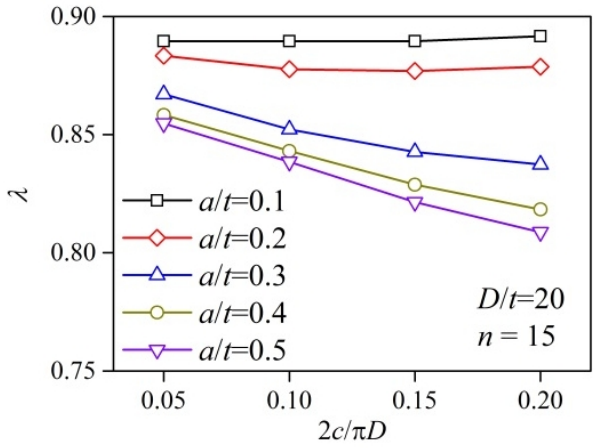

(a)

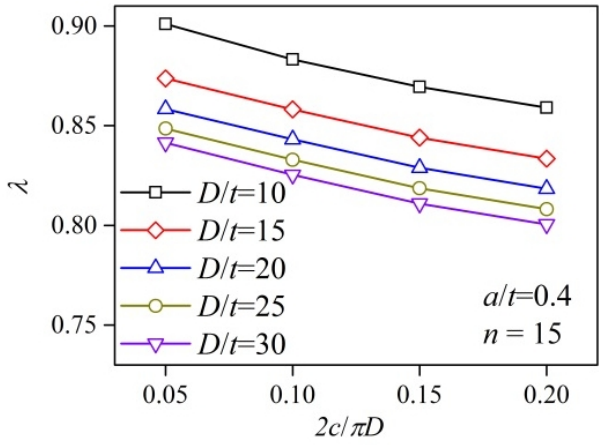

(b)

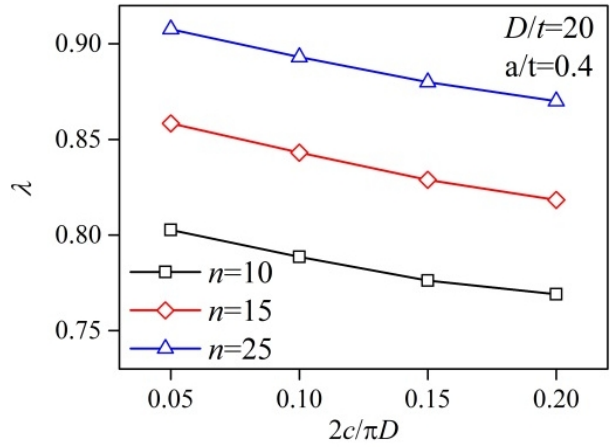

(c)

Figure 4 The interaction effect of (a) $2c/\pi D$ and a/t, (b) $2c/\pi D$ and D/t and (c) $2c/\pi D$ and n on λ.

Figure 5a shows the complex effects of D/t and a/t on λ. It can be observed that λ is almost independent of D/t for shallow cracks in contrast to that for deep cracks. As a/t increases, λ decreases significantly with

increasing D/t. A nonlinear trend is found in Fig. 5b, and $2c/\pi D$ does not change the slope of the lines; Fig. 5c also exhibits a nonlinear shape of the λ vs. D/t curve, and the descending trend becomes more modest as the strain hardening exponent increases. Figure 6 further verifies that λ is relative independent of $2c/\pi D$, D/t for shallow cracks, especially for $a/t \leq 0.1$. Therefore, it is considered that the shallow cracks have little influence on the overall compliance of a component. Moreover, it is demonstrated in Figs. 4-6 that either increasing $2c/\pi D$, D/t and a/t or decreasing n individually leads to lower λ.

It is worth noting that the normalized fracture parameter in terms of $J/(\sigma_y t)$ is independent of the yield stress, and Nourpanah and Taheri [18] have shown that the yield stress can be excluded from the investigated cracked geometries and material properties (see Table 1). Therefore, the yield stress from 400 MPa to 550 MPa is further accounted to investigate the effect of the yield stress on parameter λ. It is demonstrated in Fig. 7 that the difference of parameter λ is within 1.5% for a fixed material and crack configuration at the considered strain range, and the discrepancy decrease as the applied strain increases. Since λ is usually determined at sufficient high loads, the yield stress effect can be negligible.

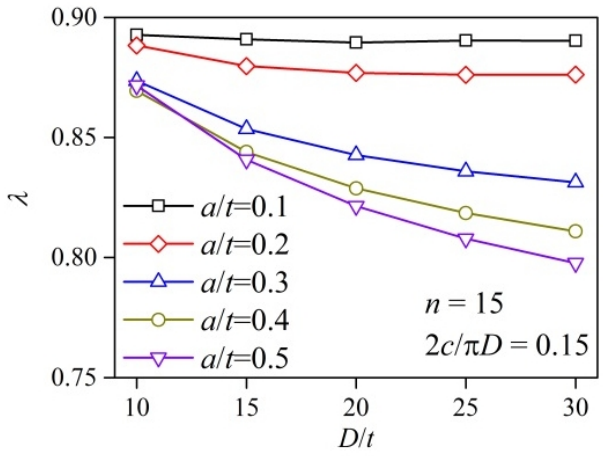

(a)

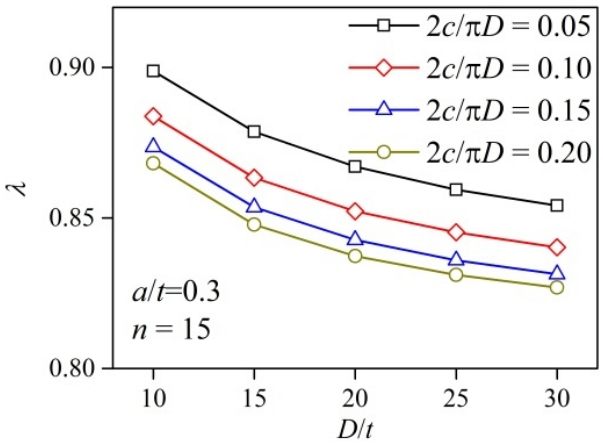

(b)

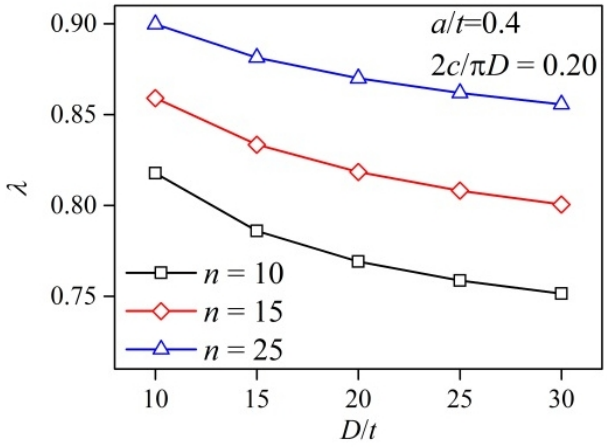

(c)

Figure 5 The interaction effect of (a) D/t and a/t, (b) D/t and $2c/\pi D$ and (c) D/t and n on λ.

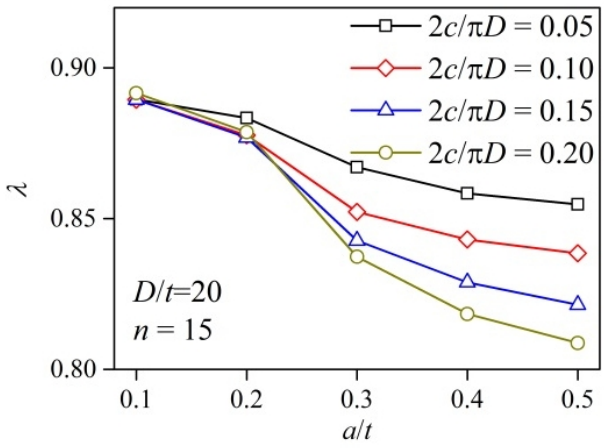

(a)

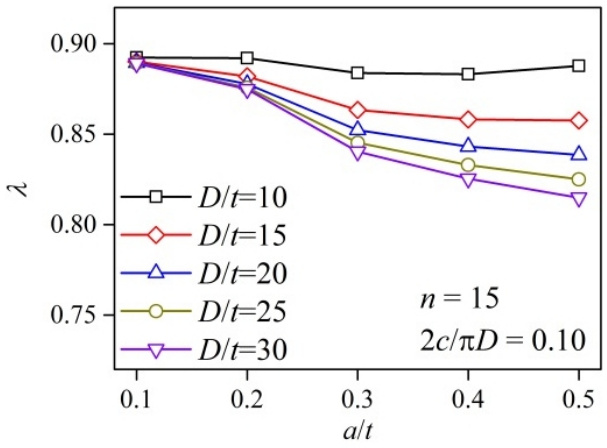

(b)

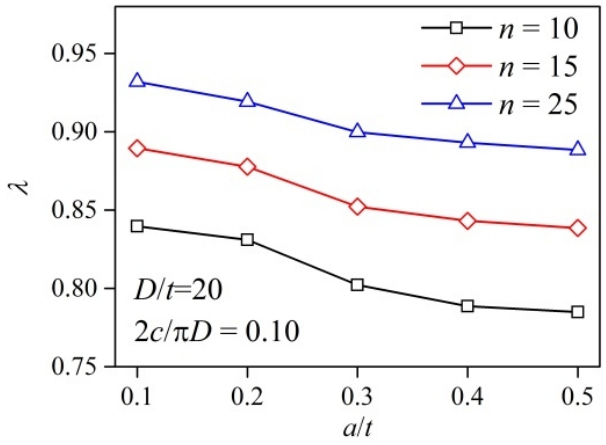

(c)

Figure 6 The interaction effect of (a) a/t and $2c/\pi D$, (b) a/t and D/t, and (c) a/t and n on λ.

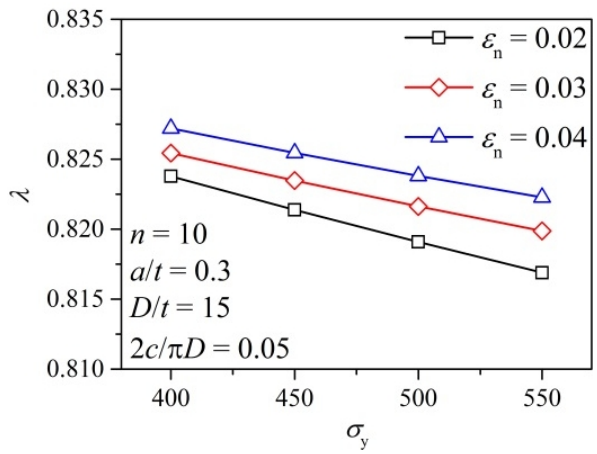

(a)

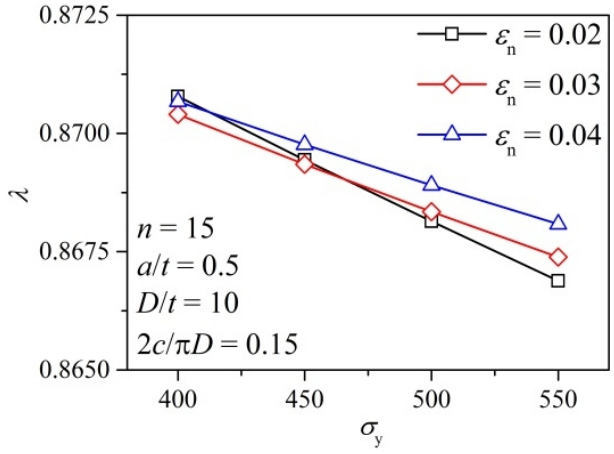

(b)

Figure 7 Effect of yield stress on λ.

For convenient application, a fitting equation is proposed based on the parametric analyses:

$$\lambda = [\beta_1\left(\frac{2c}{\pi D}\right) + \beta_2\left(\frac{D}{t}\right) + \beta_3\left(\frac{a}{t}\right) + \beta_4\left(\frac{2c}{\pi D}\right)\left(\frac{a}{t}\right) + \beta_5\left(\frac{D}{t}\right)\left(\frac{a}{t}\right) + \beta_6\left(\frac{2c}{\pi D}\right)^2 + \beta_7\left(\frac{D}{t}\right)^2 + \beta_8\left(\frac{a}{t}\right)^2 + \beta_9]\cdot n^{\beta_{10}} + \beta_0 \quad (25)$$

The coefficients fitted by the Levenberg-Marquardt (LM) method are given in Table 2, with a decisive coefficient R^2 equal to 0.98. It is worth noting that the applied range of the fitting coefficients is $10 \le D/t \le 30$, $0.1 \le a/t \le 0.5$, $0.05 \le 2c/\pi D \le 0.20$, $10 \le n \le 25$, and $0.015 \le \varepsilon_n \le 0.04$ due to the specified λ in the study.

Table 2 Fitting coefficients in Eq. (25).

β_0	β_1	β_2	β_3	β_4	β_5	β_6	β_7	β_8	β_9	β_{10}
1.1002	-0.0684	-0.0082	0.1865	-2.6559	-0.0289	1.6237	0.0003	0.4599	-0.5851	-0.4302

4. Comparison of *J* estimation schemes

In this section, the estimated *J* with the proposed reference load solution are compared against the FEA results given in Tkaczyk et al. [1]. Only five typical solutions are investigated: 1) the Kastner's limit load solution [23] recommended by BS 7910 and DNV-RP-F108 for the determination of the reference stress; 2) the modified reference stress solution of Tkaczyk et al. [1] based on the limit load solution of Kastner et al. [23]; 3) the SINTEF procedure [37, 38] developed for offshore pipes under large scale yielding during installation by S-lay or reel-lay; 4) the strain-based FAD proposed by Budden [13] using the uncracked surface strain ε_n as the reference strain ε_{ref}, and 5) the empirical formula of Jia [21] correlating the reference strain to the uncracked strain for severe cracks. The comparison is plotted in Fig. 8a for a X65 grade steel idealized with a Ramberg-Osgood fit; Fig. 8b is for a X70 steel, whose stress–strain curve includes a Lüders plateau, whereas its material response was only approximated by a Ramberg-Osgood fit (following the method proposed by Nourpanah and Taheri [18]). The agreement between the proposed *J* estimation and the FEA

results of Tkaczyk et al. [1] is reasonably good within the considered strain range. The proposed method slightly overestimates J for X70 steel due to the fitting bias of Eq. (25). It is demonstrated in Figs. 8a and 8b that the limit load solution of Kastner overestimates or underestimates J for some circumstances as indicated by Tkaczyk et al. [1]. In addition, the Kastner's limit load solution does not take the material property into account, which may have a significant influence on the determination of the limit load as demonstrated in Fig. 6c, though this solution has been generally considered to provide conservative acceptable surface breaking weld defects [1]. The SINTEF solution provides an accurate J estimation in Fig. 8a and overestimates J for X70 steel in Fig. 8b, and the discrepancy becomes noticeable as the strain increases. Budden and Ainsworth [13, 20] had pointed out that the strain-based FAD approach contained a certain degree of non-conservatism. Therefore, the crack driving force by the uncracked surface strain ε_n is observed to be the lowest line in Fig. 8. The empirical reference strain formula proposed by Jia et al. [21] is essentially derived from the strain-based J estimation

$$J(a) = J_e(a)\frac{2E\varepsilon_{ref}}{\sigma_{ref}}, \tag{26}$$

Comparing Eq. (26) with Eq. (14), it is noted that the second term in Eq. (14) is negligible in the fully plastic domain ($E\varepsilon_{ref}/\sigma_{ref} >> 1$) [39, 40], and the J estimated from Eq. (26) is then twice of that from Eq. (14). As a result, the corresponding reference strain determined from Eq. (24) and Eq. (26) is much lower than the actual reference strain for a given load level as shown in Fig. 9. Therefore, although the reference strain method modified by Jia et al. [21] is found to elevate the results of Budden et al. [13] to some extent, its estimation still underestimates J and remains a high level of non-conservatism. It is thus concluded that the proposed reference load solution is able to provide an improved estimation of J-integral for the considered geometries over the full range of interest. Moreover, the tolerable crack sizes obtained by the proposed method are examined against standard procedures for the cases considered in Fig. 8. As the cracks were assumed to be stationary, a single value of fracture toughness was used (J_c=400N/mm). For each estimation scheme, the pipe

size (Outer diameter D and the corresponding bending strain ε), the crack length ($2c$), and the crack depth (a) were altered until the crack driving force (J) reached the critical toughness, J_c. The cut-off line is chosen as $L_{r,max} = \sigma_U/\sigma_{ys}$. The predicted critical defect sizes calculated by different approaches are given in Fig. 10. BS 7910 [4] and DNV-RP-F108 [5] both adopted the limit load solution of Kastner et al. [23] for the determination of the reference stress. The results show that compared to the standardized procedure, the proposed method can give more conservative prediction of critical defect sizes, which further support the validity of the present method.

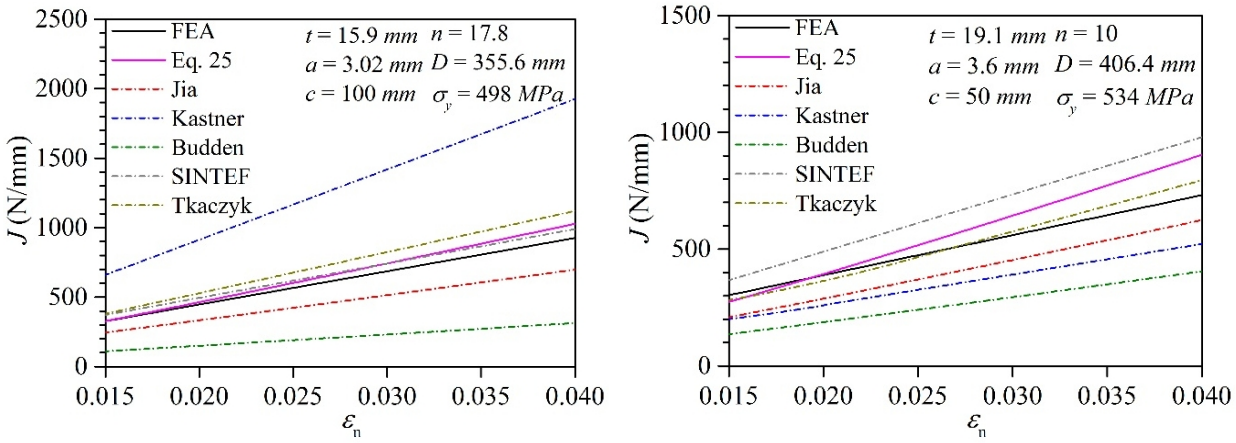

(a) (b)

Figure 8 Comparison of J estimation schemes (partially from Tkaczyk et al. [1]) with the results calculated by Eq. (25) for (a) API 5L X65 steel and (b) API 5L X70 steel following the Ramberg–Osgood model.

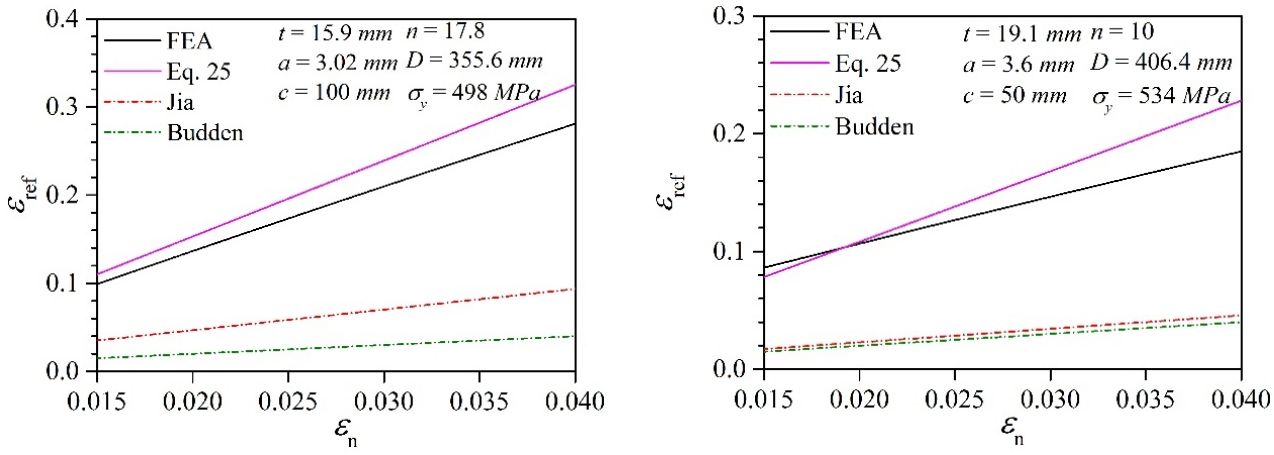

(a) (b)

Figure 9 The reference strain vs. uncracked body surface strain for (a) API 5L X65 steel and (b) API 5L X70 steel following the Ramberg–Osgood model.

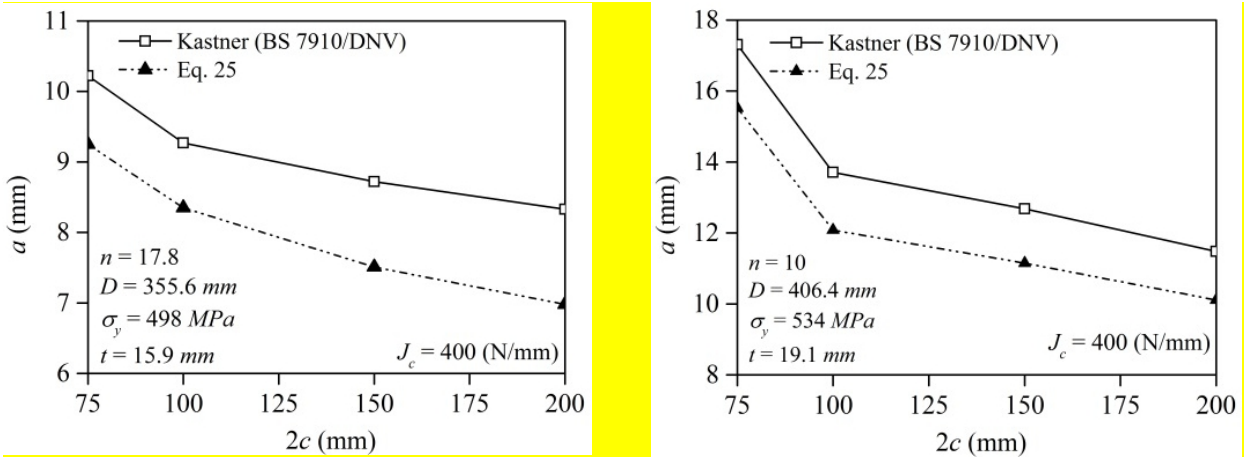

(a) (b)

Figure 10 Maximum acceptable flaw sizes for (a) API 5L X65 steel and (b) API 5L X70 steel.

5. Conclusions

In the work, an improved J estimation method is proposed to address the drawbacks of the existing J estimation schemes in circumferentially surface cracked pipes subjected to reeling. Following the EPRI methodology, a geometry and material dependent non-dimensional parameter λ is introduced to relate the reference stress directly to the uncracked remote stress. By virtual of its load-independence, an empirical

formula of λ is constructed as a function of a/t, D/t, $2c/(\pi D)$, and n. In summary, the proposed reference load solution is significantly simplified and has an explicitly theoretical foundation. Meanwhile, the comparison with the other methods in the literature indicates that the proposed crack driving force estimation of J-integral can achieve an improved accuracy for geometries over the full range of interest.

Acknowledgements

The research is financially supported by National Key Technology R&D Program of China (Grant No. 2018YFC0310306).

References

[1] Tkaczyk T, O'Dowd NP, Nikbin K. Fracture Assessment Procedures for Steel Pipelines Using a Modified Reference Stress Solution. Journal of Pressure Vessel Technology. 2009;131:031409-1.
[2] Souza RF, Ruggieri C, Zhang Z. A framework for fracture assessments of dissimilar girth welds in offshore pipelines under bending. Engineering Fracture Mechanics. 2016;163:66-88.
[3] Kyriakides S, Corona E. 1st ed. Mechanics of offshore pipelines: buckling and collapse, 1. Oxford, UK: Elsevier; 2007.
[4] BS 7910. Guide to methods for assessing the acceptability of flaws in metallic structures. London: British Standards; 2013.
[5] Det Norske Veritas. Assessment of flaws in pipeline and riser girth welds. DNVGL-RP-F108. DNV, Norway; 2017.
[6] Det Norske Veritas. Submarine pipeline systems. DNV-OS-F101. DNV, Norway; 2012.
[7] API 579-1/ASME FFS-1 2007 fitness-for-service, Second Edition, Second Edition. Washington, D.C.: American Petroleum Institute; 2007.
[8] API 1104. Welding of pipelines and related facilities, 20th edition amended July 2007. American Petroleum Institute, Washington DC; 2007.
[9] Kim Y-J, Budden PJ. Reference Stress Approximations for J and COD of Circumferential Through-Wall Cracked Pipes. International Journal of Fracture. 2002;116:195-218.
[10] Jayadevan KR, Østby E, Thaulow C. Fracture response of pipelines subjected to large plastic deformation under tension. International Journal of Pressure Vessels and Piping. 2004;81:771-783.
[11] Østby E, Jayadevan KR, Thaulow C. Fracture response of pipelines subject to large plastic deformation under bending. International Journal of Pressure Vessels and Piping. 2005;82:201-215.
[12] Budden PJ. Failure assessment diagram methods for strain-based fracture. Engineering Fracture Mechanics. 2006;73:537-552.
[13] Budden PJ, Ainsworth RA. The shape of a strain-based failure assessment diagram. International Journal of Pressure Vessels and Piping. 2012;89:59-66.
[14] Chiodo MSG, Ruggieri C. J and CTOD estimation procedure for circumferential surface cracks in pipes

under bending. Engineering Fracture Mechanics. 2010;77:415-436.
[15] Ainsworth RA. The assessment of defects in structures of strain hardening material. Engineering Fracture Mechanics. 1984;19:633-642.
[16] Anderson TL. Fracture mechanics fundamentals and applications. 3rd ed. CRC Press; 2005.
[17] Cravero S, Ruggieri C. Correlation of fracture behavior in high pressure pipelines with axial flaws using constraint designed test specimens—Part I: Plane-strain analyses. Engineering Fracture Mechanics. 2005;72:1344-1360.
[18] Nourpanah N, Taheri F. Development of a reference strain approach for assessment of fracture response of reeled pipelines. Engineering Fracture Mechanics. 2010;77:2337-2353.
[19] Linkens D, Formby CL, Ainsworth RA. A strain-based approach to fracture assessment – example applications. In: Proceedings of the fifth international conference on engineering structural integrity management, EMAS. Cambridge; 2000:45-52.
[20] Budden PJ, Smith MC. Numerical validation of a strain-based failure assessment diagram approach to fracture. In: ASME 2009 pressure vessels and piping conference. American Society of Mechanical Engineers; 2009:1797-1806.
[21] Jia P, Jing H, Xu L, Han Y, Zhao L. A modified reference strain method for engineering critical assessment of reeled pipelines. International Journal of Mechanical Sciences. 2016;105:23-31.
[22] Xiao Q, Liu Y, Dai Y. Developments of strain-based failure assessment diagram applications: measuring reference strain by displacement and a modified assessment method. International Journal of Mechanical Sciences. 2018;140:27-36.
[23] Kastner W, Röhrich E, Schmitt W, Steinbuch R. Critical crack sizes in ductile piping. International Journal of Pressure Vessels and Piping. 1981;9:197-219.
[24] Miller AG. Review of limit loads of structures containing defects. International Journal of Pressure Vessels and Piping. 1988;32:197-327.
[25] Lei Y. A review of limit load solutions for cylinders with axial cracks and development of new solutions. International Journal of Pressure Vessels and Piping. 2008;85:825-850.
[26] Zahoor, A. Ductile Fracture Handbook, Novotech Corp. 3 Volumes. 1991.
[27] Rice JR. A Path Independent Integral and the Approximate Analysis of Strain Concentration by Notches and Cracks. Journal of Applied Mechanics. 1968;35:379-386.
[28] Wells AA. Unstable crack propagation in metals: cleavage and fast fracture. In: Proceedings of the crack propagation symposium, vol. 1, Paper 84,Cranfield (UK); 1961.
[29] Hutchinson JW. Fundamentals of the Phenomenological Theory of Nonlinear Fracture Mechanics. Journal of Applied Mechanics. 1983;50:1042-1051.
[30] Hutchinson JW. Singular behaviour at the end of a tensile crack in a hardening material. Journal of the Mechanics and Physics of Solids. 1968;16:13-31.
[31] Rice JR, Rosengren GF. Plane strain deformation near a crack tip in a power-law hardening material. Journal of the Mechanics and Physics of Solids. 1968;16:1-12.
[32] Kumar V, German MD, Shih CF. An engineering approach for elastic–plastic fracture analysis. EPRI Report NP-1931. Palo Alto (CA): Electric Power Research Institute; 1981.
[33] Rahman S, Brust FW, Ghadiali N, Wilkowski GM. Crack-opening-area analyses for circumferential through-wall cracks in pipes—Part I: analytical models. International Journal of Pressure Vessels and Piping. 1998;75:357-373.
[34] Kumar V, German MD, Shih CF. An engineering approach for elastic–plastic fracture analysis. Electr Power Res Inst EPRI Report No. NP-1931, 1981.
[35] Milne, Ainsworth RA, Dowling AR, Stewart AT. Background to and validation of CEGB report R/H/R6—Revision 3. International Journal of Pressure Vessels and Piping. 1988;32:105-196.

[36] Miller AG, Ainsworth RA. Consistency of numerical results for power-law hardening materials and the accuracy of the reference stress approximation for J. Engineering Fracture Mechanics. 1989;32:233-247.
[37] Øtsby E. New strain-based fracture mechanics equations including the effects of biaxial loading, mismatch and misalignment. In: International conference on offshore mechanics and arctic engineering. Halkidiki, Greece; 2005;3:649-658.
[38] Øtsby E. Fracture Control–Offshore Pipelines Jip: Proposal for Strain-Based Fracture Assessment Procedure. In: Proceedings of the 16th International Offshore and Polar Engineering Conference.2007.
[39] Ainsworth RA. Approximate non-linear fracture mechanics calculations using reference stress techniques. In: International conference on pressure vessel and piping. 1989;170:13-19.
[40] Zerbst U, Ainsworth RA, Schwalbe KH. Basic principles of analytical flaw assessment methods. International Journal of Pressure Vessels and Piping. 2000;77:855-867.

Appendix A

Table A1 The λ factors for various material properties and cracked geometries (ε_n = 4%).

	$2c/(\pi D)$ = 0.05			$2c/(\pi D)$ = 0.1			$2c/(\pi D)$ = 0.15			$2c/(\pi D)$ = 0.2		
n	10	15	25	10	15	25	10	15	25	10	15	25
D/t = 10												
a/t												
0.1	0.8455	0.8937	0.9337	0.8443	0.8923	0.9333	0.8451	0.8927	0.9334	0.8478	0.8945	0.9344
0.2	0.8565	0.8992	0.9361	0.8490	0.8920	0.9299	0.8459	0.8883	0.9262	0.8472	0.8883	0.9257
0.3	0.8586	0.8988	0.9342	0.8424	0.8838	0.9219	0.8823	0.8735	0.9127	0.8286	0.8681	0.8790
0.4	0.8643	0.9009	0.9340	0.8421	0.8831	0.9204	0.8270	0.8694	0.9088	0.8177	0.8590	0.8997
0.5	0.8708	0.9037	0.9345	0.8515	0.8877	0.9212	0.8333	0.8716	0.9086	0.8191	0.8585	0.8996
D/t = 15												
a/t												
0.1	0.8414	0.8908	0.9322	0.8408	0.890	0.9321	0.8420	0.8908	0.9325	0.8438	0.8921	0.9333
0.2	0.8422	0.8893	0.9295	0.8361	0.8818	0.9227	0.8356	0.8797	0.9195	0.8384	0.8806	0.9194
0.3	0.8310	0.8786	0.9210	0.8158	0.8633	0.9077	0.8075	0.8535	0.8983	0.8046	0.8478	0.8914
0.4	0.8247	0.8736	0.9172	0.8077	0.8581	0.9037	0.7941	0.8439	0.8911	0.7858	0.8334	0.8813
0.5	0.8247	0.8725	0.9153	0.8098	0.8575	0.9153	0.7918	0.8407	0.8882	0.7782	0.8277	0.8882
D/t = 20												
a/t												
0.1	0.8392	0.8895	0.9314	0.8396	0.8895	0.9319	0.8411	0.8895	0.9325	0.8425	0.8916	0.9332
0.2	0.8348	0.8833	0.9256	0.8309	0.8776	0.9192	0.8328	0.8769	0.9168	0.8366	0.8787	0.9171
0.3	0.8153	0.8670	0.9133	0.8022	0.8522	0.8997	0.7954	0.8427	0.8898	0.7938	0.8373	0.8827
0.4	0.8026	0.8583	0.9076	0.7886	0.8430	0.8930	0.7762	0.8288	0.8799	0.7690	0.8183	0.8699
0.5	0.7991	0.8547	0.9038	0.7848	0.8384	0.8883	0.7673	0.8214	0.8751	0.7545	0.8087	0.8671
D/t = 25												
a/t												
0.1	0.8380	0.8887	0.9310	0.8391	0.8892	0.9318	0.8404	0.8903	0.9326	0.8419	0.8913	0.9332

0.2	0.8247	0.8736	0.9172	0.8077	0.8581	0.9037	0.7941	0.8439	0.8911	0.7858	0.8334	0.8813
0.3	0.8053	0.8593	0.9081	0.7943	0.8452	0.8943	0.7887	0.8359	0.8840	0.7882	0.8310	0.8767
0.4	0.7890	0.8485	0.9011	0.7764	0.8329	0.8854	0.7649	0.8185	0.8719	0.7586	0.8081	0.8618
0.5	0.7824	0.8425	0.8958	0.7677	0.8250	0.8789	0.7508	0.8078	0.8656	0.7387	0.7954	0.8581
$D/t = 30$												
a/t												
0.1	0.8372	0.8884	0.9309	0.8386	0.8891	0.9318	0.8401	0.8902	0.9326	0.8412	0.8910	0.9333
0.2	0.8280	0.8778	0.9215	0.8291	0.8748	0.9159	0.8332	0.8761	0.9149	0.8379	0.8789	0.9160
0.3	0.7986	0.8541	0.8903	0.7891	0.8402	0.8903	0.7847	0.8313	0.8796	0.7853	0.8269	0.8722
0.4	0.7798	0.8414	0.8962	0.7679	0.8253	0.8796	0.7570	0.8109	0.8658	0.7513	0.8004	0.8556
0.5	0.7702	0.8334	0.8895	0.7552	0.8148	0.8717	0.7388	0.7976	0.8584	0.7270	0.7853	0.8510